Reversible Chelate Ring Opening of a Sterically Crowded Palladium Bis(acyclic diaminocarbene) Complex

Yoshitha A. Wanniarachchi and LeGrande M. Slaughter*

Department of Chemistry, Oklahoma State University, Stillwater, Oklahoma 74078

Received August 29, 2007

Reaction of *cis*-dichlorobis(*p*-trifluoromethylphenylisocyanide)palladium(II) with hydrazobenzene afforded a complex with a monodentate aminohydrazino carbene ligand and an unreacted arylisocyanide. Upon heating, this complex partially converted into a chelating bis(acyclic diaminocarbene) complex. Both the monocarbene and bis(carbene) complexes were isolated and characterized by X-ray crystallography. In solution, an equilibrium between the monocarbene and bis(carbene) complexes was observed, with equilibrium constants of 2.56(15) in CD_3CN and 10.0(5) in THF-d_8 at 25 °C. A van't Hoff plot provided thermodynamic parameters of $\Delta H° = -1.7(3)$ kcal mol^{-1} and $\Delta S° = -3.7(9)$ eu for the monocarbene to bis(carbene) conversion in CD_3CN. The instability of the bis(carbene) complex toward chelate ring opening was rationalized on the basis of steric strain apparent in the X-ray structure. The crowded *syn*,*syn* arrangement of aryl groups on the bis(carbene) backbone results in widening of the carbene NCN angles to reduce aryl−aryl steric interactions. Thermodynamic calculations on density functional theory models of the carbene complexes were in reasonable agreement with experimental data, and they provided an estimate of 16 kcal mol^{-1} for the maximum amount of ligand strain that can be accommodated in forming a stable bis(carbene) ligand via diamine addition to *cis* isocyanides. The chelating bis(carbene) is thermodynamically favored despite an unfavorable reaction entropy and a substantial amount of ligand strain.

Introduction

The 1,2-addition of protic nucleophiles to coordinated isocyanides is a facile synthetic pathway to heteroatom-substituted carbene ligands.[1] This was one of the first reported routes to metal-bound diaminocarbenes,[2] which possess exceptional electronic stability among carbenes due to the presence of two strongly π-donating, σ-withdrawing nitrogen substituents on the carbene carbon.[3] Despite its historical significance and its potential for creating a new carbene in a single step, the isocyanide route has been relatively little explored as a synthetic tool for accessing structurally elaborate carbene ligands. Recently, however, the growing utility of cyclic diaminocarbenes (commonly designated N-heterocyclic carbenes or NHCs) as ligands for transition metal-based catalysis[4] has spurred renewed activity in this area. Building upon earlier work by Fehlhammer that employed β-hydroxy isocyanides as synthons for cyclic aminooxycarbene ligands,[5] Hahn and Michelin have devised facile routes to NHCs starting from isocyanides with pendent azido[6,7] or nitro[8] functionalities that serve as masked NH_2 groups. Upon coordination to the metal and in situ generation of the NH_2 moiety, these isocyanides undergo rapid nucleophilic attack to form NH,NH-substituted cyclic carbenes.[9] The latter are readily functionalized with tethering groups to form macrocyclic tetracarbene[7] or bis(phosphine)-carbene[10] ligands. A route to NHCs based on addition of propargylamine to coordinated isocyanides has also been reported.[11] Our group has been pursuing new bidentate acyclic diaminocarbene (ADC) ligands derived from isocyanides.[12–15] Isocyanide-based routes

* To whom correspondence should be addressed. E-mail: lms@chem.okstate.edu.

(1) Reviews: (a) Cotton, F. A.; Lukehart, C. M. *Prog. Inorg. Chem.* **1972**, *16*, 487–613. (b) Singleton, E.; Oosthuizen, H. E. *Adv. Organomet. Chem.* **1983**, *22*, 209–310. (c) Michelin, R. A.; Pombeiro, A. J. L.; Guedes da Silva, M. F. C. *Coord. Chem. Rev.* **2001**, *218*, 75–112.

(2) Leading references: (a) Badley, E. M.; Chatt, J.; Richards, R. L.; Sim, G. A. *Chem. Commun.* **1969**, 1322–1323. (b) Crociani, B.; Boschi, T.; Belluco, U. *Inorg. Chem.* **1970**, *9*, 2021–2025. (c) Angelici, R. J.; Charley, L. M. *J. Organomet. Chem.* **1970**, *24*, 205–209. (d) Bonati, F.; Minghetti, G.; Boschi, T.; Crociani, B. *J. Organomet. Chem.* **1970**, *25*, 255–260.

(3) Bourissou, D.; Guerret, O.; Gabbaï, F.; Bertrand, G. *Chem. Rev.* **2000**, *100*, 39–91.

(4) Reviews: (a) Herrmann, W. A. *Angew. Chem., Int. Ed.* **2002**, *41*, 1290–1309. (b) Scott, N. M.; Nolan, S. P. *Eur. J. Inorg. Chem.* **2005**, 1815–1828. (c) Hahn, F. E. *Angew. Chem., Int. Ed.* **2006**, *45*, 1348–1352.

(5) Review: (a) Tamm, M.; Hahn, F. E. *Coord. Chem. Rev.* **1999**, *182*, 175–209. (b) Leading references: Bartel, K.; Fehlhammer, W. P. *Angew. Chem., Int. Ed.* **1974**, *13*, 599–600. (c) Fehlhammer, W. P.; Bartel, K.; Plaia, U.; Völkl, A.; Liu, A. T. *Chem. Ber.* **1985**, *118*, 2235–2254. (d) Plaia, U.; Stolzenberg, H.; Fehlhammer, W. P. *J. Am. Chem. Soc.* **1985**, *107*, 2171–2172.

(6) (a) Hahn, F. E.; Langenhahn, V.; Meier, N.; Lügger, T.; Fehlhammer, W. P. *Chem. Eur. J.* **2003**, *9*, 704–712. (b) Hahn, F. E.; Langenhahn, V.; Pape, T. *Chem. Commun.* **2005**, 5390–5392. (c) Basato, M.; Benetollo, F.; Facchin, G.; Michelin, R. A.; Mozzon, M.; Pugliese, S.; Sgarbossa, P.; Sbovata, S. M.; Tassan, A. *J. Organomet. Chem.* **2004**, *689*, 454–462. (d) Basato, M.; Michelin, R. A.; Mozzon, M.; Sgarbossa, P.; Tassan, A. *J. Organomet. Chem.* **2005**, *690*, 5414–5420.

(7) Hahn, F. E.; Langenhahn, V.; Lügger, T.; Pape, T.; Le Van, D. *Angew. Chem., Int. Ed.* **2005**, *44*, 3759–3763.

(8) Hahn, F. E.; Plumed, C. G.; Münder, M.; Lügger, T. *Chem. Eur. J.* **2004**, *10*, 6285–6293.

(9) For an early example of this strategy in which the isocyanide is generated in situ from a carbonyl ligand, see: Liu, C.-Y.; Chen, D.-Y.; Lee, G.-H.; Peng, S.-M.; Liu, S.-T. *Organometallics* **1996**, *15*, 1055–1061.

(10) Kaufhold, O.; Stasch, A.; Edwards, P. G.; Hahn, F. E. *Chem. Commun.* **2007**, 1822–1824.

(11) Ruiz, J.; García, G.; Mosquera, M. E. G.; Perandones, B. F.; Gonzalo, M. P.; Vivanco, M. *J. Am. Chem. Soc.* **2005**, *127*, 8584–8585.

(12) Moncada, A. I.; Khan, M. A.; Slaughter, L. M. *Tetrahedron Lett.* **2005**, *46*, 1399–1403.

10.1021/om700866p CCC: $40.75
Publication on Web 02/29/2008

to bis(ADCs) are of interest given that ADCs have recently been reported to promote some palladium-catalyzed coupling reactions with similar activity to NHCs,[16] and standard metalation routes have proven problematic for ADCs[17] due to the decreased stability of the free carbenes.[18] Chelating bis(ADCs) date back to the first known carbene complex, which was prepared unintentionally by Chugaev in 1915 via addition of hydrazine to a platinum methyisocyanide complex[19] but was not recognized as a carbene complex until 1970.[20] We have reported that a series of palladium analogues of Chugaev's bis(carbene) complex can be readily prepared from variously substituted hydrazines and alkylisocyanides and screened to identify moderately active, air-stable Suzuki−Miyaura coupling catalysts.[12,13] More recently, we have reported the one-step syntheses of the first chiral bis(ADC) ligands via addition of chiral diamines to a palladium bis(arylisocyanide) complex,[14,15] which led to the first application of chiral ADC ligands in enantioselective catalysis.[15]

The generally facile nature of these carbene-forming reactions suggests a substantial thermodynamic driving force, presumably resulting from the formation of a new carbon−nitrogen bond. However, a few reports in the early literature indicate that nucleophilic addition of amines to isocyanides can be reversible in some cases. For amine addition to Fe^{II}−isocyanide complexes with bulky cyclopentadienyl ligands, reversible formation of monodentate ADCs has been seen in some cases even at 25 °C,[21,22] and for analogous Ru^{II} complexes equilibria between the ADC and isocyanide complexes were observed.[23] Formation of chelating bis(ADCs) from bifunctional amines is generally rapid and irreversible, with the intermediate monocarbene complex not detected. This is true for the very stable 5-membered Chugaev-type chelates (**B**, Chart 1)[12,13,20,24,25] as well as for larger chelates (**C**),[26] including the first chiral bis(ADC) (**D**) reported by us.[14] However, we found for the case of phenylhydrazine-derived palladium Chugaev carbenes that either the bis(ADC) or an uncyclized monocarbene ligand could be preferentially formed by tuning the isocyanide steric bulk.[27] Additionally, highly constrained 4-membered bis(ADC) chelates resulting from attack of primary amines on *cis* isocyanides (**A**, Chart 1) have been reported to reversibly ring-open to give monocarbene−isocyanide complexes at elevated temperatures[23,28] or upon filtration through silica gel,[29] although in no case was an equilibrium observed. The theme that emerges is that sufficient steric bulk and/or ring strain can drastically diminish the otherwise favorable driving force for carbene formation in these systems. Lacking are examples in which thermodynamic parameters for the carbene-forming nucleophilic addition can be measured and understood on the basis of ligand structural features that stabilize or destabilize the carbene moiety. This would provide valuable guidance for further development of isocyanide-based diaminocarbene ligands, as catalytically useful examples may in some cases contain substantial steric and/or ring strain. Herein we report the first example of a chelating bis(carbene) complex that is in equilibrium with the uncyclized monocarbene−isocyanide isomer in solution. Both the mono(ADC) and bis(ADC) palladium complexes have been isolated and structurally characterized. Thermodynamic parameters extracted from the temperature dependence of the equilibrium constant, along with supporting density functional theory calculations, indicate that the strong enthalpic driving force for amine addition to isocyanides favors chelating bis(carbene) formation despite an unfavorable reaction entropy and a substantial amount of steric strain in the bis(carbene) ligand.

Chart 1. Bis(ADC) Ligands

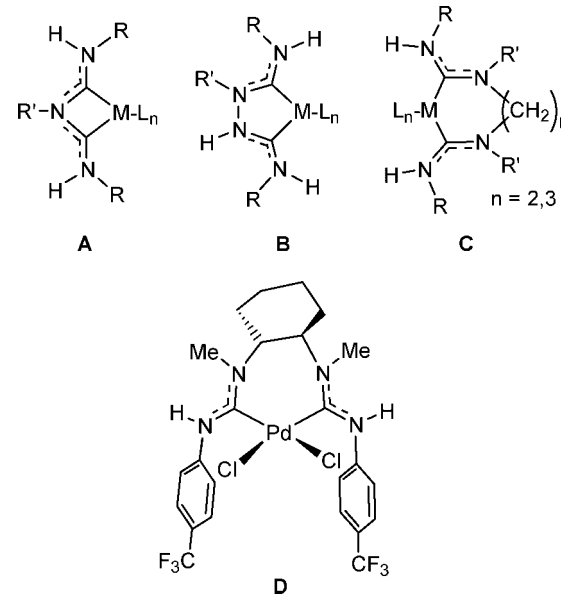

Results and Discussion

Trifluoromethyl-substituted bis(arylisocyanide) palladium dichloride complex **1** (Scheme 1) was chosen as a convenient bis(ADC) synthon, as it had previously been found to readily undergo chelative diamine addition in our synthesis of chiral bis(ADC) complex **D**.[14] We were interested in whether highly substituted Chugaev-type carbene ligands could be prepared by reaction of **1** with 1,2-disubstituted hydrazines, given that these

(13) Moncada, A. I.; Manne, S.; Tanski, J. M.; Slaughter, L. M. *Organometallics* **2006**, *25*, 491–505.
(14) Wanniarachchi, Y. A.; Slaughter, L. M. *Chem. Commun.* **2007**, 3294–3296.
(15) Wanniarachchi, Y. A.; Kogiso, Y.; Slaughter, L. M. *Organometallics* **2008**, *27*, 21–24.
(16) (a) Kremzow, D.; Seidel, G.; Lehmann, C. W.; Fürstner, A. *Chem. Eur. J.* **2005**, *11*, 1833–1853. (b) Dhudshia, B.; Thadani, A. N. *Chem. Commun.* **2006**, 668–670.
(17) (a) Herrmann, W. A.; Öfele, K.; Preysing, D. v.; Herdtweck, E. *J. Organomet. Chem.* **2003**, *684*, 235–248. (b) Herrmann, W. A.; Schütz, J.; Frey, G. D.; Herdtweck, E. *Organometallics* **2006**, *25*, 2437–2448.
(18) (a) Alder, R. W.; Blake, M. E.; Chaker, L.; Harvey, J. N.; Paolini, F.; Schütz, J. *Angew. Chem., Int. Ed.* **2004**, *43*, 5896–5911. (b) Otto, M.; Coejero, S.; Canac, Y.; Romanenko, V. D.; Rudzevitch, V.; Bertrand, G. *J. Am. Chem. Soc.* **2004**, *126*, 1016–1017.
(19) (a) Tschugajeff (Chugaev), L.; Skanawy-Grigorjewa, M. *J. Russ. Chem. Soc.* **1915**, *47*, 776. (b) Tschugajeff (Chugaev), L.; Skanawy-Grigorjewa, M.; Posnjak, A. *Z. Anorg. Allg. Chem.* **1925**, *148*, 37–42.
(20) Burke, A.; Balch, A. L.; Enemark, J. H. *J. Am. Chem. Soc.* **1970**, *92*, 2555–2557.
(21) Johnson, B. V.; Shade, J. E. *J. Organomet. Chem.* **1979**, *179*, 357–366.
(22) Fehlhammer, W. P.; Mayr, A.; Christian, G. *J. Organomet. Chem.* **1981**, *209*, 57–67.
(23) Steinmetz, A. L.; Johnson, B. V. *Organometallics* **1983**, *2*, 705–709.
(24) (a) Rouschias, G.; Shaw, B. L. *J. Chem. Soc. A* **1971**, 2097–2104. (b) Balch, A. L.; Miller, J. *J. Am. Chem. Soc.* **1972**, *94*, 417–420. (c) Butler, W. M.; Enemark, J. H.; Parks, J.; Balch, A. L. *Inorg. Chem.* **1973**, *12*, 451–457. (d) Doonan, D. J.; Balch, A. L. *Inorg. Chem.* **1974**, *13*, 921–927. (e) Lai, S.-W.; Chan, M. C. W.; Wang, Y.; Lam, H.-W.; Peng, S.-M.; Che, C.-M. *J. Organomet. Chem.* **2001**, *617–618*, 133–140.
(25) Usón, R.; Laguna, A.; Villacampa, M. D.; Jones, P. G.; Sheldrick, G. M. *J. Chem. Soc., Dalton Trans.* **1984**, 2035–2038.
(26) Fehlhammer, W. P.; Bliss, T.; Sperber, W.; Fuchs, J. *Z. Naturforsch. B* **1994**, *49*, 494–500.
(27) Moncada, A. I.; Tanski, J. M.; Slaughter, L. M. *J. Organomet. Chem.* **2005**, *690*, 6247–6251.
(28) Doonan, D. J.; Balch, A. L. *J. Am. Chem. Soc.* **1973**, *95*, 4769–4771.
(29) Sawai, T.; Angelici, R. J. *J. Organomet. Chem.* **1974**, *80*, 91–102.

Scheme 1

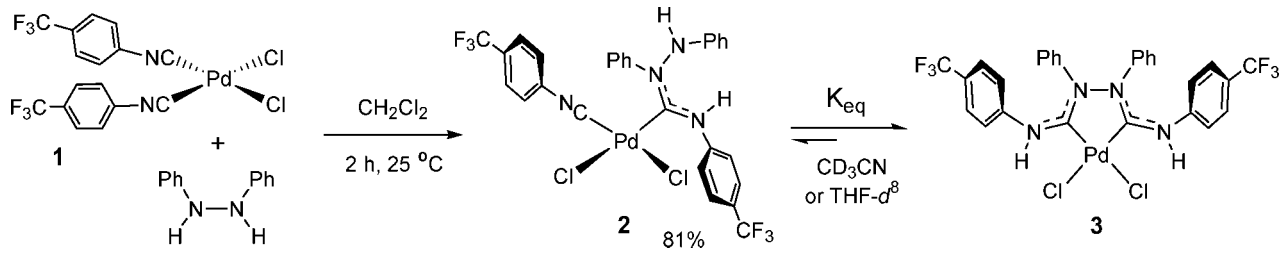

hydrazines did not afford isolable carbene complexes upon addition to palladium alkylisocyanide complexes.[30] Stirring a dichloromethane solution of **1** with 1 equiv of hydrazobenzene (1,2-diphenylhydrazine) over 2 h (Scheme 1) resulted in precipitation of a white powder that exhibited a single isocyanide stretching band at 2210 cm^{-1} when analyzed by IR spectroscopy. ^1H NMR revealed two distinct NH signals at 11.46 and 9.26 ppm and a set of aryl resonances consistent with two inequivalent phenyl groups and two inequivalent *p*-trifluoromethylphenyl groups. A ^{13}C NMR signal at 184.0 ppm was consistent with a coordinated carbene. An X-ray crystallographic analysis confirmed that the product was complex **2**, containing one monodentate aminohydrazino carbene ligand and an unreacted arylisocyanide ligand (Figure 1, Table 1). The Pd(1)−C(2) distance of 1.973(3) Å and the $C_{carbene}$−N distances of 1.334(4) and 1.332(4) Å are characteristic of a resonance-stabilized carbene ligand.[31] Complex **2** was prepared reproducibly on scales >200 mg. It is soluble in DMSO, moderately soluble in CH_3CN, and only sparingly soluble in THF and CH_2Cl_2.

Upon heating samples of **2** in CH_3CN for 5 h at 60 °C, ~60% conversion to a new product occurred, with spectroscopic signatures consistent with the chelated bis(ADC) complex **3** (Scheme 1). A single new NH resonance appeared in the ^1H NMR spectrum, and new ^1H and ^{13}C NMR signals indicated only one type each of phenyl and *p*-trifluoromethylphenyl groups in the product. The same transformation occurred in CD_3CN solutions at 25 °C, albeit more slowly. Samples of **3** that were pure by ^1H NMR in CD_2Cl_2 could be obtained by filtration of the mixture in CH_2Cl_2. Bis(carbene) complex **3** showed much higher solubility in less polar solvents such as CH_2Cl_2 and THF compared with **2**. Taking into account the varying behavior of the **2** ↔ **3** interconversion in different solvents (vide infra), we devised the following optimized synthesis of **3**. Compound **2** was heated at 60 °C in CH_3CN for 2 h to convert most of the sample to **3**, and then diethyl ether was allowed to diffuse into the solution over 2 d to gradually decrease the solvent polarity. Removal of solvent, filtration in CH_2Cl_2, and recrystallization from CH_2Cl_2/hexanes afforded **3** in 67% yield. The X-ray structure of **3** confimed a Chugaev-type bis(ADC) ligand with a five-membered chelate ring and all backbone aryl groups arranged in a mutually *syn* configuration (Figure 2, Table 2). The aryl groups are rotated away from a perpendicular disposition relative to the bis(ADC) plane with torsion angles of 13–31°, resulting in near-C_2 symmetry for the complex in the solid state.

Even carefully purified samples of **3** were found to contain small quantities of **2** that increased in concentration over time during ^1H NMR analyses in CD_3CN. Monitoring over several days established the presence of an equilibrium between monocarbene complex **2** and bis(carbene) complex **3**. The equilibrium constant at 25 °C was determined to be 2.56(15) in CD_3CN and 10.0(5) in THF-d_8. These results imply that the uncyclized monocarbene complex **2** is favored by more polar solvents. In addition, equilibrium was attained within 24 h in CD_3CN starting from pure **3** in contrast to >5 d in THF-d_8. This is consistent with the more polar solvent acting to stabilize the transition state(s) leading to the charge-separated intermediate (Figure 3) that is presumably formed in the **2** ↔ **3** interconversion. Examination of the temperature dependence of the equilibrium over the range 25 to 55 °C in CD_3CN revealed van't Hoff behavior, with K_{eq} measurably declining with increasing temperature. The van't Hoff plot (Figure 4) furnished a $\Delta H°$ of −1.7(3) kcal mol^{-1} and a $\Delta S°$ of −3.7(9) eu for the conversion of **2** to **3**. Thus, the ring-closing attack of the pendent hydrazino group of **2** on the remaining isocyanide to give **3** has a small favorable enthalpic driving force that is partially negated by entropy, yielding an overall $\Delta G°$ of −0.6(4) kcal mol^{-1} at 25 °C.

The X-ray structure of **3** displays evidence of steric strain in the bis(ADC) ligand, providing a plausible explanation for its destabilization toward chelate ring opening. The distances between *ipso* carbons of the aryl rings are 2.941(5) Å for C(11)−C(21), 2.736(5) Å for C(21)−C(31), and 2.952(6) Å for C(31)−C(41)—all substantially shorter than a carbon−carbon van der Waals contact of 3.4 Å[32]—and the *ortho*−*ortho* distances range from 3.16 to 3.40 Å. The N−$C_{carbene}$−N angles are expanded to 121.8(4)° and 123.2(3)°, as compared with the typical value of 120° for Chugaev-type carbenes,[13] evidently to minimize repulsions between the aryl groups. Further evidence of steric strain is seen in the N−N distance of 1.451(4) Å in the bis(ADC) backbone of **3**, which is elongated relative to the typical N−N distances of 1.40 Å observed in unstrained Chugaev-type bis(ADC) ligands.[13] By contrast, the aminohydrazinocarbene of **2** is rotated out of the Pd coordination plane

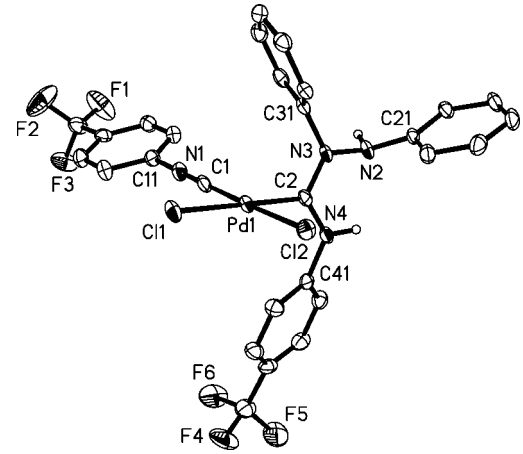

Figure 1. ORTEP view of **2** with 50% probability ellipsoids. Non-NH hydrogens are omitted for clarity.

(30) Moncada, A. I. Master's Thesis, Oklahoma State University, July 2005.

(31) (a) Herrmann, W. A.; Elison, M.; Fischer, J.; Kocher, C.; Artus, G. R. J. *Angew. Chem., Int. Ed.* **1995**, *34*, 2371–2374. (b) Ahrens, S.; Zeller, A.; Taige, M.; Strassner, T. *Organometallics* **2006**, *25*, 5409–5415.

Table 1. Selected Bond Lengths (Å) and Angles (deg) for 2

Pd−C(1)	1.926(3)
Pd−C(2)	1.973(3)
Pd−Cl(1)	2.3385(7)
Pd−Cl(2)	2.3295(8)
C(1)−N(1)	1.151(4)
C(2)−N(3)	1.334(4)
C(2)−N(4)	1.332(4)
N(2)−N(3)	1.414(3)
Pd−C(1)−N(1)	178.6(3)
C(1)−-N(1)−C(11)	178.2(3)
N(3)−C(2)−N(4)	116.1(2)
C(2)−N(3)−N(2)	119.2(2)
C(1)−Pd−C(2)	90.41(12)
C(1)−Pd−Cl(1)	90.44(9)
C(2)−Pd−Cl(2)	86.68(8)
Cl(1)−Pd−Cl(2)	92.46(3)
N(4)−C(2)−N(3)−N(2)	0.5(4)
N(4)−C(2)−N(3)−C(31)	171.0(3)
Cl(2)−Pd−C(2)−N(3)	−94.6(2)

with no steric interactions between aryl groups apparent, and the carbene has an N−$C_{carbene}$−N angle of 116.1(4)° that is typical of unstrained ADC ligands.[26,33] To the best of our knowledge, **3** is the first example of a tetrasubstituted Chugaev carbene ligand with the substituents in the highly crowded *syn*,*syn* arrangement (Figure 5). The only two other reported tetrasubstituted Chugaev carbene ligands are closely related, resulting from reaction of hydrazobenzene with *cis*-[$Au(C_6F_5)_2$-$(CNAr)_2$]ClO_4 (Ar = Ph, *p*-tolyl), but their structures were not determined.[25] It is likely that these complexes possess a less crowded *amphi*,*amphi* configuration[34] with the outer aryl substituents directed toward the Au^{III} coordination sphere (Figure 5), given that the structure of the deprotonated form of an analogous trisubstituted Chugaev carbene complex derived from phenylhydrazine and [$Au(C_6F_5)_2(CNTol)_2$]ClO_4 revealed *amphi* stereochemistry at the more substituted carbene unit.[25] In addition, a structurally similar chelating Fischer-type carbene prepared by reaction of dilithiated hydrazobenzene with $Cr(CO)_6$ followed by alkylation with [Et_3O][BF_4] displayed an *amphi*,*amphi* geometry.[35] In the case of **3**, the *amphi*,*amphi* configuration is presumably disfavored due to the steric clash that would arise between the outer aryl groups and the chloride ligands in this geometry, whereas the outer aryl in the reported Au^{III} structure could engage in a π-stacking interaction with a C_6F_5 ligand without steric interference.[25] We observed a similarly crowded *syn* configuration in a trimethyl-substituted Pd^{II} Chugaev carbene complex with *cis* bromide ligands.[13] The remarkable aspect of bis(ADC) complex **3** is that formation of the planar Chugaev-type chelate ligand is favored despite the steric strain caused by the proximity of the backbone aryl groups. No appreciable pyramidalization of the nitrogen atoms occurs to mitigate interactions between the eclipsed arene rings of **3**, with the *ipso* carbons deviating no more than 0.19 Å from the plane defined by Pd(1) and the bis(carbene) C_2N_4 backbone.

To gain insight into the thermodynamic factors favoring chelating bis(ADC) formation, we performed thermochemical calculations on models of **1**, **2**, **3**, and hydrazobenzene using density functional theory (DFT) at the B3LYP/SBK(d) level. DFT-optimized geometries of **2** and **3** accurately modeled

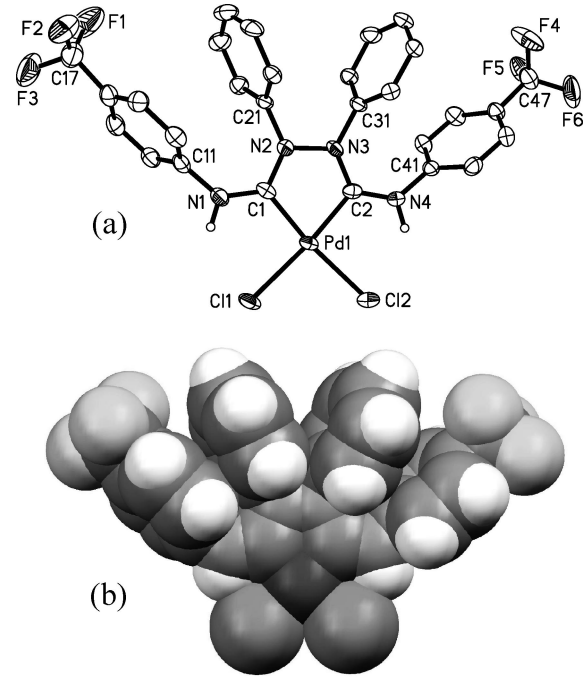

Figure 2. Two views of the molecular structure of **3**: (a) ORTEP with 50% probability ellipsoids and non-NH hydrogens removed for clarity; (b) space-filling model.

Table 2. Selected Bond Lengths (Å) and Angles (deg) for 3

Pd−C(1)	1.953(4)
Pd−C(2)	1.962(4)
Pd−Cl(1)	2.3654(9)
Pd−Cl(2)	2.3669(11)
C(1)−N(1)	1.344(5)
C(1)−N(2)	1.340(5)
C(2)−N(4)	1.334(5)
C(2)−N(3)	1.331(5)
N(2)−N(3)	1.451(4)
N(1)−C(1)−N(2)	121.8(4)
N(3)−C(2)−N(4)	123.2(3)
C(1)−Pd−C(2)	80.66(16)
C(1)−Pd−Cl(1)	93.87(11)
C(2)−Pd−Cl(2)	92.89(13)
Cl(1)−Pd−Cl(2)	92.65(4)
Pd−C(1)−N(2)−C(21)	183.0(3)
Pd−C(2)−N(3)−C(31)	174.5(3)

several important structural features of the carbene ligands (Figure 6). For the monocarbene ligand of **2**, the N−$C_{carbene}$−N angle of 115.1° closely matches the crystallographically determined value of 116.1(2)°, and the carbene C−N distances of 1.359 and 1.348 Å compare well with the experimental distances of 1.334(4) and 1.332(4) Å.[36] For bis(carbene) complex **3**, the PdC_2N_4 core is reproduced reasonably well, with Pd−$C_{carbene}$ distances of 1.987 Å (versus av. 1.958(3) Å experimental), $C_{carbene}$−N_{outer} distances of 1.341 Å (versus av. 1.339(4) Å experimental), $C_{carbene}$−N_{inner} distances of 1.379 Å (versus av. 1.336(4) Å experimental), and a backbone N−N distance of 1.461 (versus 1.451(4) experimental). However, the backbone phenyl groups are twisted away from the eclipsed arrangement

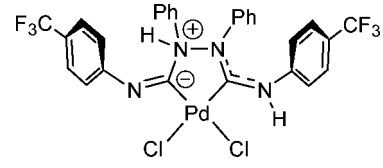

Figure 3. Plausible intermediate in the conversion of **2** to **3**.

(32) Bondi, A. *J. Phys. Chem.* **1964**, *68*, 441–451.
(33) Denk, K.; Sirsch, P.; Herrmann, W. A. *J. Organomet. Chem.* **2002**, *649*, 219–224.
(34) Miller, J.; Balch, A. L.; Enemark, J. H. *J. Am. Chem. Soc.* **1971**, *93*, 4613–4614.
(35) Hoa Tran Huy, N.; Pascard, C.; Truan Huu Dau, E.; Dötz, K. H. *Organometallics* **1988**, *7*, 590–592.

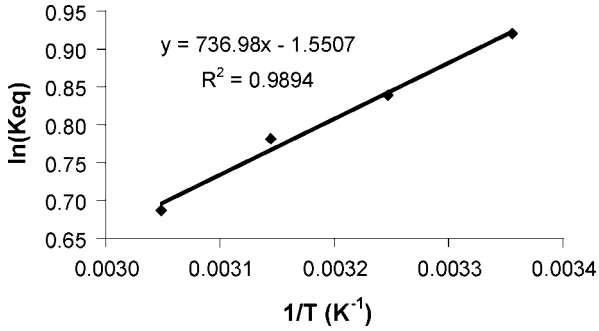

Figure 4. van't Hoff plot for the equilibrium between **2** and **3**. Data are from 25 to 55 °C.

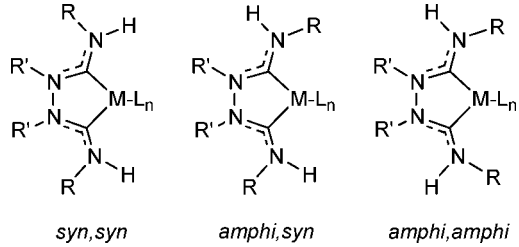

Figure 5. Possible configurations of tetrasubstituted Chugaev-type bis(ADC) ligands. For a related discussion of ADC stereochemistry, see ref 34.

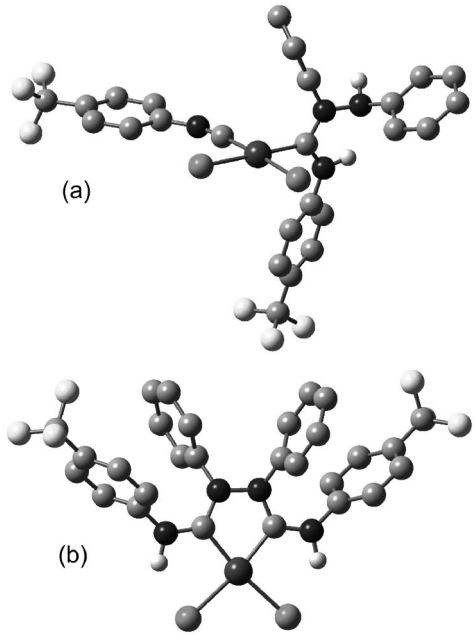

Figure 6. DFT-optimized gas-phase geometries of **2** (a) and **3** (b) at the B3LYP/SBK(d) level of theory. Relevant geometric parameters are given in the text, and a full tabulation is included in the Supporting Information.

of aryl substituents seen in the X-ray geometry, as shown by the Pd−$C_{carbene}$−N_{inner}−C_{ipso} torsion angles of 141.7°, and the $C_{carbene}$−N_{inner} distances are also somewhat elongated relative to the X-ray structure.[37] Another structural discrepancy is apparent in the DFT model of **2**, which has an elongated isocyanide C≡N bond length of 1.187 Å and a significantly bent isocyanide C≡N−C angle of 157.3°, in contrast to the respective values of 1.151(4) Å and 178.2(3)° obtained from the X-ray structure. Similarly bent isocyanides are also seen in the DFT optimized structure of **1** (see the Supporting Information). One possible explanation for these structural disparities is that the gas-phase DFT models underestimate the extent of carbon−nitrogen π-bonding in both the bound isocyanide of **2** and the bis(carbene) C_2N_4 backbone of **3**. For **2**, this could result in overestimation of metal–ligand π-backbonding with concomitant bending of the C≡N−C unit,[1b,38] whereas for **3** it could allow aryl−aryl steric interactions to perturb the N-substituents out-of-plane. The reduced N−$C_{carbene}$−N angles of 120.7° in the model of **3** (versus av. 122.5(3)° experimental) are consistent with decreased steric strain in the carbene units relative to the X-ray geometry. A second possibility is that some or all of the differences between DFT and X-ray geometries result from "soft" energy potentials that allow for easy distortion in the solid state due to crystal packing forces. To test the viability of the latter explanation, the DFT optimizations were repeated with the isocyanide Pd−C≡N and C≡N−C angles of **2** constrained to 180° and the bis(ADC) backbone of **3** constrained to planarity (all N−$C_{carbene}$−N−C_{aryl} torsion angles fixed at 0°). The constrained model of **3** optimized to a stationary point with two imaginary frequencies, but the constrained model of **2** failed to optimize after substantial computation time. Thus, the lowest energy obtained in the attempted optimization is used for **2**. The geometries of **2** and **3** obtained from these calculations are closer to the X-ray geometries than the unconstrained models (see the Supporting Information). The constrained models showed differences in electronic energy (E) relative to the unconstrained optimizations of +2 kcal mol^{-1} for **2** and +4 kcal mol^{-1} for **3**. These relatively small differences confirm that crystal packing is a plausible explanation for at least some of the observed structural discrepancies. Assuming that electronic energies dominate the enthalpy and free energy changes in this system, these calculations suggest that a difference of only 2 kcal mol^{-1} in the energy of interconversion of **2** and **3**, well within the precision of DFT methods, will result from these structural discrepancies.

Notwithstanding the modeling problems discussed above, the calculated $\Delta H°$ of −4 kcal mol^{-1} for the conversion of **2** to **3** is within 3 kcal mol^{-1} of the value of −1.7(3) kcal mol^{-1} obtained from the van't Hoff analysis, indicating that the key bonding interactions in these complexes are modeled reasonably well. Applying the +2 kcal mol^{-1} correction suggested by the constrained-geometry calculations increases the $\Delta H°$ to −2 kcal mol^{-1}, in even closer agreement with experiment. A further question was whether it was necessary to include solvent in the DFT models, given the solvent dependence of the experimentally measured **2** ↔ **3** equilibrium. Solution-phase DFT calculations utilizing the polarizable continuum model (PCM, solvent = CH_3CN)[39] or the related C-PCM model[40] at the B3LYP/SBK(d) level seemed to favor a planar, eclipsed bis(carbene) backbone in **3** very close to the X-ray geometry, but unfortunately no stable minima for **2** or **3** could be located with these methods. Single-point C-PCM calculations of the gas-phase optimized geometries were conducted, providing an estimate that the solvation of **3** in CH_3CN is more exergonic than the solvation of **2** by 0.8 kcal mol^{-1}. Combined with the computed gas-phase $\Delta G°$ of −0.5 kcal mol^{-1}, this results in

(36) A full tabulation of calculated structural parameters can be found in the Supporting Information.

(37) Gas-phase DFT calculations at the B3LYP/LANL2DZ and B3PW91/LANL2DZ levels also produced optimized geometries of **3** with pyramidalized internal nitrogens.

(38) Weber, L. *Angew. Chem., Int. Ed.* **1998**, *37*, 1515–1517.

(39) Cossi, M.; Scalmani, G.; Rega, N.; Barone, V. *J. Chem. Phys.* **2002**, *117*, 43–54.

(40) Cossi, M.; Rega, N.; Scalmani, G.; Barone, V. *J. Comput. Chem.* **2003**, *24*, 669–681.

an estimated $\Delta G°$ of -1.3 kcal mol^{-1} for the conversion of **2** to **3** in CH_3CN at 25 °C. Although this method does not allow for estimation of solvation enthalpies, the $\Delta G°$ corrections indicate that inclusion of CH_3CN solvent in the DFT models is likely to lead to a calculated $\Delta H°$ for the conversion of **2** to **3** that is slightly more exothermic than the gas-phase estimate but still reasonably close to the experimental value. The remainder of the discussion will assume that the gas-phase enthalpies derived from unconstrained calculations are sufficiently accurate for meaningful conclusions to be drawn.

The primary enthalpic driving force for the cyclization of **2** to give **3** is undoubtedly the creation of a new carbon−nitrogen bond, which has a bond strength of at least 69–75 kcal mol^{-1} based on data for C−N single bonds.[41] This driving force is mitigated by two factors: (1) the overall decrease in carbon−nitrogen π-bonding on conversion of the isocyanide into a carbene, and (2) strain energy resulting from the constrained Chugaev-type chelate ring and steric interactions of the eclipsed aryl groups. The DFT-calculated gas-phase $\Delta H°$ for the reaction of bis(isocyanide) complex **1** with hydrazobenzene to form unstrained monocarbene complex **2** is -20 kcal mol^{-1}, providing a benchmark enthalpic driving force that reflects only the carbene-forming bond rearrangments with no significant contribution from strain energy. In combination with the calculated $\Delta H°$ for conversion of **2** to **3**, this provides an estimate of 16 kcal mol^{-1} for the strain energy present in the sterically crowded bis(ADC) complex **3**. Given the nature of the **2** ↔ **3** equilibrium, this value can be considered an approximate upper limit on the amount of strain energy that can be accommodated while still favoring formation of a stable bis(ADC) chelate by attack of a bifunctional amine on *cis*-coordinated isocyanides.

A striking feature of this approach to the synthesis of chelating bis(carbene) ligands is that the enthalpic driving force is sufficiently strong to overcome unfavorable entropic factors. Because no ligands are released upon chelative addition of a diamine to *cis*-isocyanides, the entropic advantage associated with the classical chelate effect does not apply to these reactions.[42] This is illustrated by the calculated $\Delta S°$ value of -50 eu for the reaction of **1** with hydrazobenzene to give **2**, which is inferred from the DFT-computed $\Delta H°$ (-20 kcal mol^{-1}) and $\Delta G°$ (-5 kcal mol^{-1} at 25 °C) for this reaction. Combining this with the experimental $\Delta H°$ and $\Delta S°$ for the cyclization of **2** to **3** affords thermodynamic parameters for the overall reaction **1** + hydrazobenzene → **3** as follows: $\Delta H° = -22$ kcal mol^{-1}, $\Delta S° = -50$ eu, and $\Delta G° = -6$ kcal mol^{-1}. For comparison with an example of a bis(ADC) ligand that does not exhibit strained carbene moieties, the corresponding parameters for our previously reported reaction of **1** with *trans*-*N*,*N*′-dimethyl-1,2-diaminocyclohexane to form chiral bis(ADC) complex **D** (Chart 1)[14] are $\Delta H° = -32$ kcal mol^{-1}, $\Delta S° = -67$ eu, and $\Delta G° = -12$ kcal mol^{-1} as calculated from DFT models at the B3LYP/SBK(d) level (see the Supporting Information). It is possible that electronic factors contribute to the weaker driving force for **3** given that arylamines showed a greater tendency for reversibility in ADC formation than alkylamines in one report,[22] but the conspicuous strain present in the structure of **3** argues for steric factors playing the dominant role.

(41) Smith, M. B.; March, J. *March's Advanced Organic Chemistry*, 5th ed.; Wiley: New York, 2001; pp 22–24..

(42) Huheey, J. E.; Keiter, E. A.; Keiter, R. L. *Inorganic Chemistry*, 4th ed.; HarperCollins: New York, 1993; pp 522–531..

Conclusion

The stepwise formation of complex **3** represents the first example of an isocyanide-derived bis(ADC) in which both the intermediate monocarbene−isocyanide complex and the chelating bis(carbene) product have been isolated and structurally characterized, as well as the first example of a directly observed equilibrium between these two species. Structural analysis of **3** implicates strain in the carbene moieties resulting from steric interactions between backbone aryl groups as a likely cause of the instability of the bis(ADC) ligand toward chelate ring opening. However, formation of the planar Chugaev-type bis(ADC) backbone of **3** is still thermodynamically favored despite the eclipsed arrangement of aryl groups that results from planarization. This suggests that π-bonding within the NCN units contributes substantially to the stability of the bis(ADC) ligand, although crystal packing forces cannot be ruled out as a factor favoring ligand planarity. The strong enthalpic driving force for formation of a bis(ADC) ligand is sufficient to overcome unfavorable entropic factors and considerable ligand strain energy, up to 16 kcal mol^{-1} as judged by DFT calculations. This bodes well for the effectiveness of amine addition to isocyanides as a strategy for the synthesis of structurally elaborate cyclic or acyclic carbene ligands, but it illustrates that there is a limit to the amount of steric or ring strain that can be accommodated in fashioning a stable ligand by this route.

Experimental Section

General Considerations. All manipulations were performed under vacuum or nitrogen in dry solvents unless otherwise noted. Anhydrous acetonitrile was purchased in septum-sealed bottles from Acros and used as received. Dichloromethane (Pharmco) was washed with concentrated H_2SO_4, water, and aqueous $NaHCO_3$, and then distilled from P_2O_5 prior to use. Hexanes (Pharmco) and diethyl ether (Acros) were distilled from Na/benzophenone ketyl prior to use. NMR solvents were purchased from Cambridge Isotope Laboratories. CD_3CN and DMSO-d_6 were dried by stirring over activated 4Å molecular sieves and then vacuum distilled at room temperature. CD_2Cl_2 was dried similarly and then stored over and distilled from P_2O_5 before use. THF-d_8 was dried over and distilled from Na/benzophenone ketyl prior to use. Hydrazobenzene (Aldrich) was recrystallized from hot EtOH under Ar and stored in a nitrogen glovebox to avoid air oxidation to azobenzene. Compound **1** was prepared as previously reported.[14] NMR spectra were recorded on Varian GEMINI 2000 (300 MHz) and Varian Unity INOVA (400 and 600 MHz) spectrometers. Reported chemical shifts are referenced to residual solvent peaks (^{13}C, ^{1}H) or to calibrated external standards (^{19}F). IR spectra were acquired from KBr pellets on a Nicolet Protégé 460 FT-IR spectrometer. Elemental analyses were performed by Desert Analytics, Tucson, Arizona. J Young NMR tubes used for equilibrium measurements were flame-dried under active vacuum before use.

Synthesis of Palladium Monocarbene Complex (2). To a solution of **1** (200 mg, 0.385 mmol) in 20 mL of CH_2Cl_2 in a sealable flask was added hydrazobenzene (78 mg, 0.423 mmol). The flask was sealed with a Teflon stopcock, and the reaction mixture was stirred under nitrogen for 2 h at 25 °C. Product **2** formed as a white precipitate, which was filtered through a fine frit under air, washed with 5 mL of CH_2Cl_2, and dried under vacuum for 12 h. Yield 218 mg, 81%. ^{1}H NMR (300 MHz, DMSO-d_6) δ 11.46 (1H, s, N*H*), 9.26 (1H, s, N*H*), 8.07–7.98 (4H, 2 d overlapped, CF_3−Ph), 7.92–7.82 (4H, 2 m overlapped, Ph), 7.77 (2H, d, J = 8.1 Hz, CF_3−Ph), 7.53–7.44 (2H, m, Ph), 7.42–7.36 (1H, m, Ph *para*), 7.28–7.20 (2H, m, Ph), 6.96 (2H, d, J = 7.8 Hz, CF_3−Ph), 6.90–6.83 (1H, m, Ph *para*). ^{13}C NMR (75 MHz, DMSO-d_6) d 184.0 (carbene), 144.2 (Ar), 143.8 (Ar), 143.4 (Ar), 131.3 (Ar),

131.1 (Ar), 129.1 (Ar), 128.6 (Ar), 127.8 (Ar), 127.4 (q, $^3J_{CF}$ = 3.6 Hz, CF_3−Ph *meta*), 126.8 (Ar), 126.1 (Ar), 125.9 (q, $^3J_{CF}$ =3.6 Hz, CF_3−Ph *meta*), 121.2 (Ar), 114.5 (Ar). ArN*C*, *C*F_3, and CF_3−Ph *para* not detected. Longer acquistion times did not allow detection of these peaks due to rapid decomposition of **2** in DMSO-d_6, and **2** was insufficiently soluble in other solvents. ^{19}F NMR (282 MHz, DMSO-d_6) δ –60.5, –61.4. IR (KBr pellet) ν_{max}/cm^{-1} 2210. Anal. Calcd for $C_{28}H_{20}N_4F_6Cl_2Pd$: C, 47.78, H, 2.86, N, 7.96. Found: C, 47.56, H, 2.73, N, 7.98.

Synthesis of Palladium Bis(Carbene) Complex (3). Monocarbene complex **2** (200 mg, 0.284 mmol) was placed in a sealable flask with 5 mL of anhydrous CH_3CN, and the mixture was stirred at 60 °C under nitrogen for 2 h. The cooled reaction mixture was transferred into a vial in the glovebox, and diethyl ether was allowed to slowly diffuse into the solution over 2 d. The solvent was then removed under reduced pressure, and 5 mL of CH_2Cl_2 was added. The mixture was stirred to dissolve as much solid as possible, and the CH_2Cl_2 was distilled off in vacuo. This process was repeated twice more to remove any residual CH_3CN. The solid residue was then taken up in 5 mL of CH_2Cl_2 and filtered through a fine frit to remove any unconverted starting material. The small amount of solid on the frit was washed with an additional 3 mL of CH_2Cl_2, and the clear filtrate was concentrated under reduced pressure. Addition of hexanes to this filtrate caused precipitation of a pale yellow powder, which was dried under vacuum for 12 h. Yield 133 mg, 67%. ^{1}H NMR (300 MHz, CD_2Cl_2) δ 10.51 (2H, s, N*H*), 7.09 (8H, AB, J = 8.6 Hz, C = 14.6 Hz, CF_3−Ph *ortho*,*meta*), 6.95–6.92 (2H, m, Ph *para*), 6.83–6.76 (8H, m, Ph *ortho*,*meta*). ^{13}C NMR (150 MHz, CD_2Cl_2) δ 183.0 (carbene), 140.82 (q, $^4J_{CF}$ = 1.2 Hz, CF_3−Ph *ortho*), 136.87 (CF_3−Ph *ipso*), 131.18 (Ph *ipso*), 130.63 (Ph), 129.34 (q, $^2J_{CF}$ = 32.8 Hz, CF_3−Ph *para*), 129.2 (Ph), 127.21 (Ph), 125.82 (q, $^3J_{CF}$ = 3.7 Hz, CF_3−Ph *meta*), 123.80 (q, $^1J_{CF}$ = 272 Hz, *C*F_3). ^{19}F NMR (282 MHz, CD_2Cl_2) δ −63.6. Anal. Calcd for $C_{28}H_{20}N_4F_6Cl_2Pd$: C, 47.78, H, 2.86, N, 7.96. Found: C, 48.11, H, 3.03, N, 7.84.

Equilibrium Measurements. Into a flame-dried J Young NMR tube was added **3** (1.6 mg, 2.3 μmol). The tube was evacuated, and 0.6 mL of NMR solvent (CD_3CN or THF-d_8) was added by vacuum distillation. The NMR tube was placed in a calibrated Fisher Isotemp 210 constant temperature water bath set at 25.0 °C. ^{19}F NMR spectra were acquired every 1–2 days until equilibrium had been reached as judged by integral ratios of the respective CF_3 peaks. To ensure accurate integrations of NMR signals, acquisition times of 5 s and delay times (d1) of 3 s were employed. Relaxation times for the CF_3 ^{19}F NMR signals were determined to be in the range 1.15–1.30 s by the inversion–recovery method. Uncertainties are reported at the 95% confidence level. These were determined from concurrent analyses of triplicate samples at 2 d for CD_3CN, and for three successive analyses on the same sample for THF-d_8 starting at 13 d and separated by 2 d.

Van't Hoff Analysis. A sample of **3** (8 mg, 11 μmol) was placed in a vial with 0.6 mL of freshly distilled CD_3CN, and the mixture was agitated with a pipet to form a saturated solution of **3**. The mixture was filtered through a fine frit, and the filtrate was placed in a flame-dried J Young NMR tube. The tube was placed in a calibrated constant temperature water bath, and ^{19}F NMR spectra were acquired at temperatures of 25, 35, 45, and 55 °C, with the sample allowed to equilibrate for 2 d in the water bath prior to each NMR analysis. The NMR probe was also set to the desired temperature prior to each data acquisition (probe temperature calibrated). NMR acquisition parameters were the same as those used for the room temperature equilibrium measurements. Slow degradation of **2/3** was observed at 55 °C with concomitant precipitation of a small amount of yellow solid, and significantly faster degradation above 60 °C prohibited collection of additional data points. An equilibrium experiment starting from **2** could not be successfully completed due to accelerated degradation of **2** at higher initial concentrations, which was accompanied by precipitation of possibly polymeric solid material in the tube. Uncertainties in thermodynamic quantities were derived from the least-squares linear regression analysis of the K_{eq} temperature dependence and are reported at the 95% confidence level.

X-ray Crystal Structure Determinations. Crystals of **2** and **3** obtained by slow evaporation of CH_3CN solutions of the respective compounds were immersed in Paratone N oil in a Nylon loop and placed in the coldstream of a Bruker SMART APEX II diffractometer at 100(2) K. In the case of **2**, roughly half of the crystals screened were determined to be **3** by indexing. Diffraction data were collected with use of graphite-monochromated Mo Kα radiation (λ = 0.71073 Å) via a series of φ and ω scans, with 0.5° scan widths and 30 s exposure times. Data integration employed the SAINT software package, and multiscan absorption corrections were applied with SADABS.[43] Structures were solved by direct methods and refined by full-matrix least-squares on F^2, using the SHELXTL software suite.[44] All non-hydrogen atoms were refined anisotropically, and all hydrogens (except H(2) in **2**) were placed in calculated positions (riding model) with isotropic U fixed at 1.2 times the U_{eq} of the attached atom. The hydrazino NH of **2** (H(2)) was restrained to a distance of 0.92(1) Å from N(2) with its other positional parameters allowed to refine freely. For **2**, difference Fourier peaks clustered about inversion centers at fractional coordinates 0,½,0 and 0,1,½ were suggestive of solvent molecules disordered in multiple orientations. The SQUEEZE procedure[45] in PLATON[46] was used to treat the disorder, and the model was consistent with two CH_3CN molecules (42 e$^-$/unit cell). Crystal data for **2**: $C_{28}H_{20}Cl_2F_6N_4Pd$, fw = 703.78, crystal size 0.21 × 0.14 × 0.02 mm^3, monoclinic, $P2_1/c$, a = 10.4570(8) Å, b = 22.908(2) Å, c = 12.7945(11) Å, β = 93.873(5)°, U = 3057.9(4) Å^3, Z = 4, μ = 0.842 mm^{-1}, $2\theta_{max}$ = 28.3°, 33056 total reflections, 7575 independent (R_{int} = 0.069). Final R1 [$I > 2\sigma(I)$] = 0.0432, wR2 (all data) = 0.0926. Crystal data for **3**: $C_{28}H_{20}Cl_2F_6N_4Pd$, fw = 703.78, crystal size 0.11 × 0.06 × 0.06 mm^3, triclinic, $P1^-$, a = 9.0014(5) Å, b = 11.4002(6) Å, c = 14.6460(7) Å, α = 110.666(3)°, β = 93.013(3)°, γ = 100.034(3)°, U = 1374.07(12) Å^3, Z = 2, μ = 0.937 mm^{-1}, $2\theta_{max}$ = 26.4°, 10778 total reflections, 5572 independent (R_{int} = 0.063). Final R1 [$I > 2\sigma(I)$] = 0.0477, wR2 (all data) = 0.1175. These structures have been deposited at the Cambridge Crystallographic Data Centre and assigned the following deposition numbers: (**2**) CCDC 658516 and (**3**) CCDC 658517.

Computational Details. Density functional theoretical (DFT) calculations were performed with the GAUSSIAN03 quantum chemistry package,[47] using the B3LYP hybrid functional.[48] Pal-

(43) *APEX2 software suite (SAINT, SADABS)*, Version 2.0; Bruker AXS: Madison, WI, 2006.

(44) Sheldrick, G. M. *SHELXTL, Version 6.14*; Bruker AXS Inc.: Madison, WI, 2000.

(45) van der Sluis, P.; Spek, A. L. *Acta Crystallogr., Sect. A* **1990**, *46*, 194–201.

(46) Spek, A. L. *PLATON, A Multipurpose Crystallographic Tool*; Utrecht University: Utrecht, The Netherlands, 2007.

(47) Frisch, M. J.; Trucks, G. W.; Schlegel, H. B.; Scuseria, G. E.; Robb, M. A.; Cheeseman, J. R.; Montgomery, J. A.; Vreven, T.; Kudin, K. N.; Burant, J. C.; Millam, J. M.; Iyengar, S. S.; Tomasi, J.; Barone, V.; Mennucci, B.; Cossi, M.; Scalmani, G.; Rega, N.; Petersson, G. A.; Nakatsuji, H.; Hada, M.; Ehara, M.; Toyota, K.; Fukuda, R.; Hasegawa, J.; Ishida, M.; Nakajima, T.; Honda, Y.; Kitao, O.; Nakai, H.; Klene, M.; Li, X.; Knox, J. E.; Hratchian, H. P.; Cross, J. B.; Bakken, V.; Adamo, C.; Jaramillo, J.; Gomperts, R.; Stratmann, R. E.; Yazyev, O.; Austin, A. J.; Cammi, R.; Pomelli, C.; Ochterski, J. W.; Ayala, P. Y.; Morokuma, K.; Voth, G. A.; Salvador, P.; Dannenberg, J. J.; Zakrzewski, V. G.; Dapprich, S.; Daniels, A. D.; Strain, M. C.; Farkas, O.; Malick, D. K.; Rabuck, A. D.; Raghavachari, K.; Foresman, J. B.; Ortiz, J. V.; Cui, Q.; Baboul, A. G.; Clifford, S.; Cioslowski, J.; Stefanov, B. B.; Liu, G.; Liashenko, A.; Piskorz, P.; Komaromi, I.; Martin, R. L.; Fox, D. J.; Keith, T.; Al-Laham, M. A.; Peng, C. Y.; Nanayakkara, A.; Challacombe, M.; Gill, P. M. W.; Johnson, B.; Chen, W.; Wong, M. W.; Gonzalez, C.; Pople, J. A. *GAUSSIAN 03*, Revision C.02; Gaussian, Inc.: Wallingford, CT, 2004.

ladium and main group elements were described by using the relativistic effective core potentials (ECPs) and valence basis sets (VBSs) of Stevens,[49] denoted CEP-31G in GAUSSIAN03. The valence basis sets of heavy main group elements were augmented with d polarization functions by using the Extrabasis keyword, with exponents of 0.8 for C, N, and F and an exponent of 0.75 for Cl. This ECP/VBS combination, denoted SBK(d) in the literature, has been used in combination with suitable DFT methods to reliably model structural and energetic properties of a wide range of transition metal organometallic complexes,[50] including a chiral palladium bis(ADC) complex (**D**, Chart 1) reported by us.[14]

For complexes **2** and **3**, DFT geometry optimizations were performed by using atomic coordinates from the X-ray structures as input geometries. For complex **1** and hydrazobenzene, the molecule builder function of GAUSSVIEW[51] was employed to create reasonable starting geometries, which were submitted for geometry optimization and frequency calculations at the B3LYP/SBK(d) level of theory. For **1**, the starting geometry had linear Pd−C≡N angles and aryl rings perpendicular to the coordination plane. Optimizations were performed on all degrees of freedom, and all gas-phase optimized structures were verified as true minima with no imaginary frequencies, with the exception of the constrained-geometry calculations mentioned in the Results and Discussion. For the latter calculations, geometric constraints were specified by using the ModRedundant keyword in GAUSSIAN03. Calculated thermodynamic quantities utilized unscaled vibrational frequencies derived from the energy Hessian, with the temperature specified as 298.15 K. Solvent-phase calculations used the polarizable continuum model (PCM),[52] as revised by Cossi and co-workers,[39] or the related conductor-like PCM model (C-PCM),[40] with CH_3CN as solvent ($\epsilon = 36.64$). The calculated "(polarized solute)-solvent" energies from single-point C-PCM calculations of **2** and **3** in CH_3CN were utilized to convert gas-phase $\Delta G°$ values for the **2** ↔ **3** interconversion into solvent-phase estimates (calculated solvation free energy for **2** = −42.4 kcal mol^{-1}; for **3**, −43.2 kcal mol^{-1}).

Acknowledgment. We thank the Donors of the American Chemical Society Petroleum Research Fund (40196-G1) and the National Science Foundation (CAREER Award CHE-0645438) for funding. The Oklahoma State Regents for Higher Education furnished funds for purchase of the APEX II diffractometer. Some of the DFT calculations were performed using the resources of the Center for Advanced Scientific Computing and Modeling (CASCaM) at the University of North Texas, which is supported by a grant from the U.S. Department of Education. Dr. Tom Cundari (University of North Texas) provided valuable computational advice and access to CASCaM resources.

Supporting Information Available: Computational details and calculated geometries, representative NMR spectra of **2**, **3**, and the equilibrium mixture, and crystallographic data for **2** and **3** in CIF format. This material is available free of charge via the Internet at http://pubs.acs.org.

OM700866P

(48) (a) Becke, A. D. *J. Chem. Phys.* **1993**, *98*, 5648–5652. (b) Lee, C.; Yang, W.; Parr, R. G. *Phys. Rev.* **1998**, *B37*, 785–789.

(49) Krauss, M.; Stevens, W. J.; Basch, H.; Jasien, P. G. *Can. J. Chem.* **1992**, *70*, 612–630.

(50) (a) Benson, M. T.; Cundari, T. R.; Lutz, M. L.; Sommerer, S. O. In *Reviews in Computational Chemistry*; Boyd, D., Lipkowitz, K., Eds.; Wiley: New York, 1996; Vol. 8, pp 145–202. (b) Veige, A. S.; Slaughter, L. M.; Lobkovsky, E. B.; Wolczanski, P. T.; Matsunaga, N.; Decker, S. A.; Cundari, T. R. *Inorg. Chem.* 2003, *42*, 6204–6224. (c) Bergman, R. G.; Cundari, T. R.; Gillespie, A. M.; Gunnoe, T. B.; Harman, W. D.; Klinckman, T. R.; Temple, M. D.; White, D. P. *Organometallics* **2003**, *22*, 2331–2337.

(51) Dennington, R.; Keith, T.; Millam, J.; Eppinnett, K.; Hovell, W. L.; Gilliland, R. *GAUSSVIEW*, Version 3.08; Semichem, Inc.: Shawnee Mission, KS, 2003.

(52) Amovilli, C.; Barone, V.; Cammi, R.; Cances, E.; Cossi, M.; Mennucci, B.; Pomelli, C.; Tomasi, J. *Adv. Quantum Chem.* **1999**, *32*, 227–261.